Journal of Sound and Vibration (1997) **203**(1), 101–126

A FOURIER SERIES APPROACH TO THE MEASUREMENT OF FLEXURAL WAVE INTENSITY IN PLATES

C. R. HALKYARD

Industrial Research Ltd., P.O. Box 2225, *Auckland, New Zealand*

AND

B. R. MACE

Department of Mechanical Engineering, University of Auckland, Private Bag 92019, *Auckland, New Zealand*

(*Received* 9 *June* 1995, *and in final form* 7 *November* 1996)

In regions sufficiently remote from excitation and discontinuities, the flexural motion of a plate can be expressed as the sum of plane propagating waves. In this paper this fact is used as the basis of a wave-based technique for plate intensity measurement. It is assumed that far field conditions exist, and that the displacement within a region can be described as the sum of a set of plane waves the amplitude of which is a function of propagation direction. This function is approximated using a truncated complex Fourier series. It is shown that the time-averaged intensity at the co-ordinate origin can be written in terms of the five Fourier coefficients of lowest order. The effect that the choice of measured variables and measurement locations have on systematic errors and on the conditioning of the problem is discussed. A numerical comparison, under specific conditions, between a Fourier series approach and a finite difference approach to plate intensity measurement is shown. This indicates that the Fourier series approach can offer a better compromise between systematic and random errors. Experimental intensity measurements illustrating the use of the Fourier series approach are presented and discussed.

1. INTRODUCTION

The measurement of vibrational energy flow, or *intensity*, in structures has received considerable attention from researchers since its proposal by Noiseux [1], and there is no doubt that the idea of structural intensity measurement is an appealing one, particularly for the analysis of noise and vibration problems in complex structures. It offers a unifying concept by which different vibration types in different structural members can be compared and ranked. Once the relative importance of the various sources, vibration types and transmission paths are known, the selection of effective vibration treatment is greatly simplified. Examples of specific applications of structural intensity measurements are given in references [2, 3].

Expressions for flexural wave intensity in beams and plates in terms of variables that can be readily measured [4] have been known for many years. There can, however, be many problems involved in practical intensity measurements. In practice, the intensity is estimated from the local deformation (i.e., displacement, velocity and their spatial derivatives of various orders) of the structural member. This deformation is generally determined from measurements at a finite number of locations at and around the point

0022–460X/97/210101 + 26 $25.00/0/sv960854

of interest, which involves, explicitly or implicitly, fitting functions to the measured data and finding the "deformation" of these functions.

If the relationship between the internal stresses and the external deformation is known, the maximum achievable accuracy of the intensity estmate will be dependent on how well the functions used to interpolate between the measurement points represent the deformation of the structural member. This is determined both by the types of function used and the spacing of the measurement points. If the functions perfectly match the deformation there will be no systematic error in the intensity estimate provided that certain spacings, which result in matrix singularity, are avoided. If, however, the interpolating functions do not match the deformation there will inevitably be a systematic error which increases with an increasing spacing between the measurement points.

Although systematic errors can be minimized through the use of a small spacing (in terms of wavelengths) between the measurement points, such a measurement system will be sensitive to errors in the input data. This can be readily appreciated when one considers the effects of errors in measurements or transducer placement on the estimate of the deformed shape if the measurement points are closely spaced, and thus the measured variables are near-identical. The sensitivity of a calculation to errors in the input data is termed the *conditioning* of the problem, with a well conditioned problem being relatively insensitive to errors.

If the conditioning of the intensity calculation is improved then the effects of measurement errors are reduced. This potentially allows for better intensity estimates, or permits measurements to be performed in more demanding conditions than would otherwise be possible. Improved conditioning can generally be achieved through the use of more widely spaced measurement points (up to a certain limit, after which the conditioning deteriorates again), but unless the true and assumed deformations are in close agreement it can be at the expense of large systematic errors. The use of appropriate functions to interpolate between the measurement points is therefore fundamental to achieving a good compromise between systematic errors and conditioning.

In the calculation of flexural wave intensity, the spatial derivatives of displacement in beams and plates have traditionally been estimated using finite difference approximations [4–7], which implicitly fit low order polynomials of position to the measured data. In general these functions do not agree closely with the true deformation over a wide domain, and therefore their use can result in substantial systematic errors if the measurement points are not closely spaced [8–10]. More suitable interpolating functions are thus desirable.

Within the limits of thin beam theory, the displacement of a flexurally vibrating beam can be expressed in terms of propagating and evanescent waves. The deformation can thus be represented exactly using trigonometric and exponential functions. The technique of wave decomposition, in which the wave amplitudes are determined, fits these functions to the measured data, and beam intensity measurements based on this technique [11–13] therefore can avoid systematic errors. A small separation between measurement points is thus not necessary, and the spacing may be chosen purely to give low sensitivity to measurement errors.

In contrast, there does not exist a general closed form solution to the equation of motion of a plate. It is thus not possible to select interpolating functions that, in a finite expansion, exactly represent the deformation. As a consequence, any system for plate intensity measurement that utilizes a finite number of measurement locations will result in a systematic error. However, through the use of suitable interpolating functions, systematic errors and/or the sensitivity of the intensity calculation to measurement and other errors can be reduced.

It is shown in the following section that, in a region remote from discontinuities and excitation, the displacement of a plate can be approximated as the sum of plane propagating waves. Functions of this form would therefore appear to be an appropriate choice of interpolating function for far field plate intensity measurements. This paper describes such a measurement system, in which it is assumed that the plate displacement can be written as the sum of plane waves the amplitude of which is a function of propagation direction. The amplitude function is expressed as a complex Fourier series which is truncated to allow the Fourier coefficients to be estimated from a finite number of measurements. The intensity can be calculated directly from the Fourier coefficients.

In section 3 the displacement of a plate is approximated in terms of a truncated Fourier series. This approximation is used in section 4 to derive an expression for the intensity in terms of the Fourier coefficients. The principles of estimating the Fourier coefficients and the geometry of possible transducer arrays are discussed in section 5. In section 6 the effects that the choice of measured variables and measurement locations have on the conditioning of the problem is described. Simulated intensity measurements, using Fourier series and finite difference based approaches, are compared in terms of systematic errors and sensitivity to measurement errors in sections 7 and 8 respectively. Finally, the results of experimental intensity measurements using the Fourier series approach are presented and discussed in section 9.

2. PLATE RESPONSE IN TERMS OF PLANE WAVES

Consider an infinite plate, with elastic modulus E, density ρ, Poisson ratio v, and thickness h, excited by the time-harmonic point force $f(r, \phi, t) = F\delta(r)\,\mathrm{e}^{\mathrm{i}\omega_0 t}$ acting normal to the plate surface (a list of symbols used is given in Appendix 2). Within the limitations of thin plate theory, which apply to isotropic, homogeneous flat plates the thickness of which is small relative to a wavelength and the displacement of which is small relative to the thickness of the plate, it can be shown that the equation of motion is given by [14]

$$D\nabla^2\nabla^2 w(r, \phi, t) - \rho h\omega_0^2 w(r, \phi, t) = f(r, \phi, t), \tag{1}$$

where

$$D = \frac{Eh^3}{12(1 - v^2)} \tag{2}$$

is the flexural stiffness per unit width of the plate and ∇^2 is the Laplace operator. The response of the plate at a distance, r, from the excitation point is given by [14]

$$w(r, t) = \frac{-\mathrm{i}F\,\mathrm{e}^{\mathrm{i}\omega_0 t}}{8k_p^2 D}\,[\mathrm{H}_0^{(2)}(k_p r) - \mathrm{H}_0^{(2)}(-\mathrm{i}k_p r)], \tag{3}$$

where

$$k_p = \sqrt[4]{\frac{\omega_0^2 \rho h}{D}} \tag{4}$$

is the plate wavenumber and

$$\mathrm{H}_0^{(2)}(k_p r) = \mathrm{J}_0(k_p r) - \mathrm{i}\mathrm{Y}_0(k_p r) \tag{5}$$

is the zeroth order Hankel function of the second kind.

The displacement field of an infinite plate excited by a time-harmonic point force can thus be written in terms of the difference of two Hankel functions, the one with a real

argument (assuming that $k_p r$ is purely real) representing radially propagating waves and the one with an imaginary argument representing the near-field effects. Expressions of this form can be considered the Green functions for time-harmonic bending waves in a plate, with the applied forces and boundary conditions of an arbitrary plate being described as the sum of a number of point sources. This gives an expression for the displacement of an infinite plate under the resulting force distribution, however the displacements in the interior domain are identical to those of the finite plate.

Further simplification is possible if only regions remote from excitation and discontinuities are considered. In these cases the arguments of the Hankel functions are large, and it is known that, for large z, [15]

$$H_0^{(2)}(z) \approx \sqrt{\frac{2}{\pi z}}\, e^{-i(z-\pi/4)}. \tag{6}$$

It is immediately apparent that if the argument has a negative imaginary component then exponential decay with distance occurs, with the magnitude of this imaginary component determining the rate of decay. The presence of structural damping introduces a negative imaginary component to the wavenumber, meaning that the arguments of both Hankel functions in equation (3) have negative imaginary components. However, in most structural materials the loss factor is very small, making the wavenumber almost purely real. Under these circumstances the argument $(k_p r)$ has a relatively small imaginary component, while that of $(-ik_p r)$ is relatively large. As a consequence only the Hankel function, $H_0^{(2)}(k_p r)$, is significant at large r. Equation (3) therefore becomes

$$w(r, t) \approx \frac{-iF\, e^{i\omega_0 t}}{8k_p^2 D} \sqrt{\frac{2}{\pi k_p r}}\, e^{-i(k_p r - \pi/4)}. \tag{7}$$

Now consider a section, S, of the plate surface, upon which the excitation can be represented by a distribution of point sources $F(x_0, y_0)$. If (x', y') represents the point of interest on the plate, then the radial distance of this point from the sources is

$$r(x_0, y_0) = \sqrt{(x' - x_0)^2 + (y' - y_0)^2}, \tag{8}$$

and provided that $k_p r$ is large the displacement at point (x', y') is given by

$$w(x', y', t) \approx \iint_S \frac{-iF(x_0, y_0)\, e^{i\pi/4}\, e^{i\omega_0 t}}{8k_p^2 D} \sqrt{\frac{2}{\pi k_p r(x_0, y_0)}}\, e^{-ik_p r(x_0, x_0)}\, dx_0\, dy_0. \tag{9}$$

Furthermore, if the dimensions of the area of excitation, S, are small relative to r, then $1/\sqrt{r(x_0, x_0)}$ may be considered constant over S, and equation (9) may be rewritten as

$$w(x', x', t) \approx \frac{-i\, e^{i\pi/4}\, e^{i\omega_0 t}}{8k_p^2 D} \sqrt{\frac{2}{\pi k_p r}} \iint_S F(x_0, y_0)\, e^{-ik_p r(x_0, y_0)}\, dx_0\, dy_0. \tag{10}$$

At the point (x', y') this may be interpreted as a set of plane waves emanating from region S in the direction of (x', y'). If boundaries and sources of excitation are sufficiently remote from the point of interest then each may be represented by a number of such regions. Furthermore, within a small vicinity of point (x', y') there will be little variation in r, and thus a very similar wave description applies throughout that vicinity. The response at, and

within a vicinity of, point (x', y') can therefore be expressed as the sum of the contributions of the individual regions and hence as the sum of plane waves from various directions.

3. WAVE AMPLITUDE AS A COMPLEX FOURIER SERIES

It was seen in the previous section that, within the vicinity of a point, sufficiently remote from discontinuities or excitation and which we will arbitrarily denote the co-ordinate origin, the displacement of a plate can be approximated as the sum of plane propagating waves. These waves may be of any direction, so the displacement can be written as

$$w(x, y) \approx \int_{-\pi}^{\pi} A(\theta)\, \mathrm{e}^{-\mathrm{i}k_p(x\cos\theta + y\sin\theta)}\, \mathrm{d}\theta, \tag{11}$$

where $A(\theta)$ is the complex wave amplitude as a function of propagation direction, θ. Writing this amplitude as a complex Fourier series gives

$$A(\theta) = \sum_{n=-\infty}^{\infty} C_n\, \mathrm{e}^{\mathrm{i}n\theta}. \tag{12}$$

Equation (12) can then be substituted in equation (11) to yield

$$w(x, y) \approx \int_{-\pi}^{\pi} \left(\sum_{n=-\infty}^{\infty} C_n\, \mathrm{e}^{\mathrm{i}n\theta} \right) \mathrm{e}^{-\mathrm{i}k_p(x\cos\theta + y\sin\theta)}\, \mathrm{d}\theta, \tag{13}$$

or

$$w(x, y) \approx \sum_{n=-\infty}^{\infty} C_n \int_{\pi}^{\pi} \mathrm{e}^{\mathrm{i}n\theta}\, \mathrm{e}^{-\mathrm{i}k_p(x\cos\theta + y\sin\theta)}\, \mathrm{d}\theta. \tag{14}$$

While there are an infinite number of terms in the Fourier series expansion, in practice the displacement will be estimated from a finite number of measurements, m. It is therefore possible to estimate up to m coefficients in the expansion. If m is odd then we may write $m = 2q + 1$ for some non-negative integer, q, and the estimate of displacement given by the truncated Fourier series approximation is

$$\bar{w}(x, y) \approx \sum_{n=-q}^{q} C_n \int_{-\pi}^{\pi} \mathrm{e}^{\mathrm{i}n\theta}\, \mathrm{e}^{-\mathrm{i}k_p(x\cos\theta + y\sin\theta)}\, \mathrm{d}\theta. \tag{15}$$

4. INTENSITY IN TERMS OF COMPLEX FOURIER COEFFICIENTS

Subject to the limitations of thin plate theory, which are paraphrased in section 2, the components of time-averaged flexural wave intensity in the x- and y-directions can be shown to be [4]

$$\langle I_x(t)\rangle = D\left[\left\langle \left(\frac{\partial^3 w}{\partial x^3} + \frac{\partial^3 w}{\partial x\, \partial y^2} \right) \frac{\partial w}{\partial t} \right\rangle - \left\langle \left(\frac{\partial^2 w}{\partial x^2} + \nu \frac{\partial^2 w}{\partial y^2} \right) \frac{\partial^2 w}{\partial x\, \partial t} \right\rangle - (1-\nu) \left\langle \frac{\partial^2 w}{\partial x\, \partial y} \frac{\partial^2 w}{\partial y\, \partial t} \right\rangle \right] \tag{16}$$

and

$$\langle I_y(t)\rangle = D\left[\left\langle\left(\frac{\partial^3 w}{\partial x^2\,\partial y}+\frac{\partial^3 w}{\partial y^3}\right)\frac{\partial w}{\partial t}\right\rangle-\left\langle\left(v\frac{\partial^2 w}{\partial x^2}+\frac{\partial^2 w}{\partial y^2}\right)\frac{\partial^2 w}{\partial y\,\partial t}\right\rangle-(1-v)\left\langle\frac{\partial^2 w}{\partial x\,\partial y}\frac{\partial^2 w}{\partial x\,\partial t}\right\rangle\right] \tag{17}$$

where $\langle\ \rangle$ denotes a time average. In the far field it is known that

$$\frac{\partial^2 w}{\partial x^2}+\frac{\partial^2 w}{\partial y^2}=-k_p^2 w, \tag{18}$$

and therefore, for far field conditions, equations (16) and (17) can be rewritten as

$$\langle I_x(t)\rangle = D\left[\left\langle -k_p^2\frac{\partial w}{\partial x}\frac{\partial w}{\partial t}\right\rangle-\left\langle\left(\frac{\partial^2 w}{\partial x^2}+v\frac{\partial^2 w}{\partial y^2}\right)\frac{\partial^2 w}{\partial x\,\partial t}\right\rangle-(1-v)\left\langle\frac{\partial^2 w}{\partial x\,\partial y}\frac{\partial^2 w}{\partial y\,\partial t}\right\rangle\right], \tag{19}$$

$$\langle I_y(t)\rangle = D\left[\left\langle -k_p^2\frac{\partial w}{\partial y}\frac{\partial w}{\partial t}\right\rangle-\left\langle\left(v\frac{\partial^2 w}{\partial x^2}+\frac{\partial^2 w}{\partial y^2}\right)\frac{\partial^2 w}{\partial y\,\partial t}\right\rangle-(1-v)\left\langle\frac{\partial^2 w}{\partial x\,\partial y}\frac{\partial^2 w}{\partial x\,\partial t}\right\rangle\right]. \tag{20}$$

In order to evaluate equations (19) and (20), it is necessary to estimate spatial derivatives of displacement of up to second order. This may be achieved by differentiating equation (15) to give

$$\begin{aligned}
w(x,y) &\approx \sum_{n=-q}^{q} C_n\int_{-\pi}^{\pi} \mathrm{e}^{\mathrm{i}n\theta}\,\mathrm{e}^{-\mathrm{i}k_p(x\cos\theta+y\sin\theta)}\,\mathrm{d}\theta,\\
\frac{\partial w}{\partial x}(x,y) &\approx \sum_{n=-q}^{q} C_n\int_{-\pi}^{\pi} -\mathrm{i}k_p\cos\theta\,\mathrm{e}^{\mathrm{i}n\theta}\,\mathrm{e}^{-\mathrm{i}k_p(x\cos\theta+y\sin\theta)}\,\mathrm{d}\theta,\\
\frac{\partial w}{\partial y}(x,y) &\approx \sum_{n=-q}^{q} C_n\int_{-\pi}^{\pi} -\mathrm{i}k_p\sin\theta\,\mathrm{e}^{\mathrm{i}n\theta}\,\mathrm{e}^{-\mathrm{i}k_p(x\cos\theta+y\sin\theta)}\,\mathrm{d}\theta,\\
\frac{\partial^2 w}{\partial x\partial y}(x,y) &\approx \sum_{n=-q}^{q} C_n\int_{-\pi}^{\pi} -k_p^2\cos\theta\sin\theta\,\mathrm{e}^{\mathrm{i}n\theta}\,\mathrm{e}^{-\mathrm{i}k_p(x\cos\theta+y\sin\theta)}\,\mathrm{d}\theta,\\
\frac{\partial^2 w}{\partial x^2}(x,y) &\approx \sum_{n=-q}^{q} C_n\int_{-\pi}^{\pi} -k_p^2\cos^2\theta\,\mathrm{e}^{\mathrm{i}n\theta}\,\mathrm{e}^{-\mathrm{i}k_p(x\cos\theta+y\sin\theta)}\,\mathrm{d}\theta,\\
\frac{\partial^2 w}{\partial y^2}(x,y) &\approx \sum_{n=-q}^{q} C_n\int_{-\pi}^{\pi} -k_p^2\sin^2\theta\,\mathrm{e}^{\mathrm{i}n\theta}\,\mathrm{e}^{-\mathrm{i}k_p(x\cos\theta+y\sin\theta)}\,\mathrm{d}\theta.
\end{aligned} \tag{21}$$

Since the spatial derivatives given in equations (21) are functions of location, it is possible to estimate the intensity at any point in the region over which the proposed wave description remains valid. Under these circumstances, when x and y are non-zero, the integrals in equations (21) are typically non-zero and thus all the calculated coefficients, C_n, contribute to the intensity estimate. However, at the co-ordinate origin, where $x = y = 0$, the position dependent exponential term simply equals unity, and the

orthogonality of trigonometric functions means that the integrals are zero for most values of n. The displacement and its relevant spatial derivatives given in equations (21) are therefore, at the co-ordinate origin, determined by a small number of coefficients; namely,

$$w(0,0) \approx 2\pi C_0, \qquad \frac{\partial w}{\partial x}(0,0) \approx -\mathrm{i}k_p\pi(C_{-1} + C_1),$$

$$\frac{\partial w}{\partial y}(0,0) \approx k_p\pi(-C_{-1} + C_1), \qquad \frac{\partial^2 w}{\partial x \partial y}(0,0) \approx \frac{\mathrm{i}k_p^2\pi}{2}(C_{-2} - C_2),$$

$$\frac{\partial^2 w}{\partial x^2}(0,0) \approx -k_p^2\pi[0{\cdot}5(C_{-2} + C_2) + C_0], \qquad \frac{\partial^2 w}{\partial y^2}(0,0) \approx k_p^2\pi[0{\cdot}5(C_{-2} + C_2) - C_0]. \quad (22)$$

Substituting equations (22) into equations (19) and (20) gives, as estimates of time-averaged intensity in the x- and y-directions,

$$\langle I_x(t)\rangle_{FS} = \frac{D\omega k_p^3}{2}\pi^2 \,\mathrm{Re}\,[2C_0(C_{-1} + C_1)^* + (1 - \nu)(C_{-2}^* C_{-1} + C_2^* C_1) + (1 + \nu)C_0^*(C_{-1} + C_1)], \quad (23)$$

and

$$\langle I_y(t)\rangle_{FS} = \frac{D\omega k_p^3}{2}\pi^2 \,\mathrm{Im}\,[2C_0(C_1 - C_{-1})^* + (1 - \nu)(C_2^* C_1 - C_{-2}^* C_{-1}) + (1 + \nu)C_0^*(C_{-1} - C_1)], \quad (24)$$

if the wavenumber, k_p, is purely real. Five coefficients are thus sufficient to determine the intensity at the origin under far field conditions.

Adaptation of the intensity calculation to allow for damping poses no problems, through the use of a complex stiffness, D, and wavenumber, k_p. Note, however, that it is the local damping within the material that is important, rather than the overall damping of the structure (which may be dominated by losses at joints, boundaries, etc., and is likely to be much higher than the material damping [14]). The effect of damping within the material is to change the phase relationships between the velocities and internal forces that are used to estimate the intensity, and results in expressions for intensity similar to, but rather more complex than, equations (23) and (24). If the damping is high in the region of the measurement—due, for example, to the use of constrained layer damping—the inclusion of damping in this manner may be warranted. For typical levels of material damping, however, the assumption of a purely real wavenumber will not result in a significant error in the intensity estimate.

5. ESTIMATION OF FOURIER SERIES COEFFICIENTS

The Fourier coefficients may be estimated from measurements of displacement made at different points by solving a set of simultaneous equations of the form given in equation (15). These equations can be rewritten in terms of matrices as

$$\mathbf{W} = \mathbf{TC}, \quad (25)$$

where

$$\mathbf{T} = \begin{bmatrix} \displaystyle\int_{-\pi}^{\pi} \mathrm{e}^{-\mathrm{i}q\theta}\, \mathrm{e}^{-\mathrm{i}k_p(x_1\cos\theta + y_1\sin\theta)}\,\mathrm{d}\theta & \cdots & \displaystyle\int_{-\pi}^{\pi} \mathrm{e}^{\mathrm{i}q\theta}\, \mathrm{e}^{-\mathrm{i}k_p(x_1\cos\theta + y_1\sin\theta)}\,\mathrm{d}\theta \\ \vdots & & \vdots \\ \displaystyle\int_{-\pi}^{\pi} \mathrm{e}^{-\mathrm{i}q\theta}\, \mathrm{e}^{-\mathrm{i}k_p(x_m\cos\theta + y_m\sin\theta)}\,\mathrm{d}\theta & \cdots & \displaystyle\int_{-\pi}^{\pi} \mathrm{e}^{\mathrm{i}q\theta}\, \mathrm{e}^{-\mathrm{i}k_p(x_m\cos\theta + y_m\sin\theta)}\,\mathrm{d}\theta \end{bmatrix},$$

$$\mathbf{C}^{\mathrm{T}} = (C_{-q} \cdots C_q), \qquad \mathbf{W}^{\mathrm{T}} = (w(x_1, y_1) \cdots w(x_m, y_m)), \tag{26}$$

and thus the Fourier coefficients may be estimated from

$$\mathbf{C} = \mathbf{T}^{-1}\mathbf{W}. \tag{27}$$

Similar formulations can be derived for measured variables other than displacement.

If the number of measurements exceeds the number of coefficients being evaluated, then the Moore–Penrose inverse may be used to obtain a least squares fit to the measured data [16]. However, for the remainder of the paper it will be assumed, unless specifically stated, that the number of measurements is equal to the number of Fourier coefficients.

The effects of damping may be included through the use of a complex wavenumber, k_p. However, for this to yield a significantly improved estimate of the Fourier coefficients, the decay of the waves as they propagate across the region occupied by the transducer array, which is governed by the material loss factor and the dimensions of the array, must be measurable.

The basis functions used in the complex Fourier series possess angular periodicity, and therefore the angular placement of the transducers used to estimate the coefficients must be appropriate for that purpose. This is analogous to the choice of a suitable linear spacing of transducers when evaluating wave amplitudes in a beam [13]. In practice, it is necessary to avoid angular spacings which coincide with a half-period of one of the basis functions, since this results in singularity of the matrix, $\mathbf{T}$, used to evaluate the Fourier coefficients. This behaviour is apparent from the determinant of the matrix. Changing to polar co-ordinates, with

$$x = \hat{r}\cos\hat{\phi}, \qquad y = \hat{r}\sin\hat{\phi}, \tag{28}$$

equation (15) becomes

$$w(\hat{r}, \hat{\phi}) \approx \sum_{n=-p}^{q} c_n \int_{-\pi}^{\pi} \mathrm{e}^{\mathrm{i}n\theta}\, \mathrm{e}^{-\mathrm{i}k_p\hat{r}(\cos\hat{\phi}\cos\theta + \sin\hat{\phi}\sin\theta)}\,\mathrm{d}\theta = \sum_{n=-q}^{q} C_n\, \mathrm{e}^{\mathrm{i}n\hat{\phi}} \int_{-\pi}^{\pi} e^{\mathrm{i}n\theta}\, \mathrm{e}^{-\mathrm{i}k_p\hat{r}\cos\theta}\,\mathrm{d}\theta. \tag{29}$$

Now consider m measurements of displacement (or velocity or acceleration) taken at points on the circumference of a circle of radius, R, with uniform angle, φ, between adjacent measurement points, as shown in Figure 1. It can be shown from equation (29) that the elements of the transformation matrix, $\mathbf{T}$, are given by

$$\mathbf{T}_{j,s_n} = \mathrm{e}^{\mathrm{i}n(j-1)\varphi} \int_{-\pi}^{\pi} \mathrm{e}^{\mathrm{i}n\theta}\, \mathrm{e}^{-\mathrm{i}k_pR\cos\theta}\,\mathrm{d}\theta = \mathrm{e}^{\mathrm{i}n(j-1)\varphi} U_n, \tag{30}$$

where

$$U_n = \int_{-\pi}^{\pi} \mathrm{e}^{\mathrm{i}n\theta}\, \mathrm{e}^{-\mathrm{i}k_pR\cos\theta}\mathrm{d}\theta = 2\pi(-\mathrm{i})^n \mathrm{J}_n(k_pR) \tag{31}$$

and s_n is the column of matrix, $\mathbf{T}$, associated with Fourier index n, J_n being the nth order Bessel function of the first kind. As U_n is independent of the angular location of the measurement, it is constant for any column of the matrix. Furthermore, since multiplying a row or column of a matrix by a constant factor has the effect of changing the determinant by that same factor, the zeroes of the determinant of the matrix, $\mathbf{T}$, are the same as the zeroes for the auxiliary matrix, $\bar{\mathbf{T}}$, where

$$\bar{\mathbf{T}}_{j,\,s_n} = \mathrm{e}^{in(j-1)\varphi} \tag{32}$$

or, letting $b = \mathrm{e}^{i\varphi}$,

$$\bar{\mathbf{T}} = \begin{bmatrix} 1 & \cdots & 1 & 1 & 1 & \cdots & 1 \\ b^{-q} & \cdots & b^{-1} & 1 & b & \cdots & b^{q} \\ b^{-2q} & \cdots & b^{-2} & 1 & b^{2} & \cdots & b^{2q} \\ \vdots & \cdots & \vdots & \vdots & \vdots & \cdots & \vdots \\ b^{-q(m-1)} & \cdots & b^{-(m-1)} & 1 & b^{(m-1)} & \cdots & b^{q(m-1)} \end{bmatrix}. \tag{33}$$

Zeroes of the determinant of matrix, $\bar{\mathbf{T}}$, indicate angular spacings that will result in singularity of matrix $\mathbf{T}$. It is apparent in this case that any uniform angular spacing may be used provided that it does not result in two measurements occurring at the same location, since singularity occurs only when

$$\varphi = 2\pi, \ldots, \pm\frac{2\pi}{(m-2)}, \quad \pm\frac{2\pi}{(m-1)}. \tag{34}$$

A measurement system with all tranducers evenly spaced around the circumference of a circle would therefore appear to be a practical proposition. If, however, one measurement is taken at the centre, the elements of the row of matrix, $\mathbf{T}$, associated with this measurement are of the form

$$\begin{aligned} \int_{-\pi}^{\pi} \mathrm{e}^{in\theta}\,\mathrm{d}\theta &= 0 \qquad (\forall n \neq 0) \\ &= 2\pi \qquad (n = 0). \end{aligned} \tag{35}$$

Thus only the central element of the row is non-zero, with the Fourier coefficient, C_0, being fully determined by this single measurement. The auxiliary matrix, $\bar{\mathbf{T}}$, now has the form

$$\bar{\mathbf{T}} = \begin{bmatrix} 0 & \cdots & 0 & 1 & 0 & \cdots & 0 \\ 1 & 1 & \cdots & 1 & \cdots & 1 & 1 \\ b^{-q} & b^{-(q-1)} & \cdots & 1 & \cdots & b^{(q-1)} & b^{q} \\ b^{-2q} & b^{-2(q-1)} & \cdots & 1 & \cdots & b^{2(q-1)} & b^{2q} \\ \vdots & \vdots & \cdots & \vdots & \cdots & \vdots & \vdots \\ b^{-q(m-2)} & b^{-(q-1)(m-2)} & \cdots & 1 & \cdots & b^{(q-1)(m-2)} & b^{q(m-2)} \end{bmatrix}. \tag{36}$$

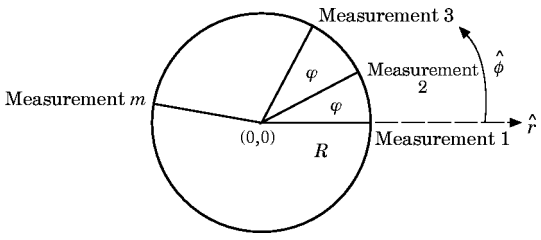

Figure 1. The transducer arrangement for Fourier series approximation.

Singularity occurs at the same angular spacings as in the previous case. In this situation, however, there are only $(m-1)$ tranducers arranged circumferentially. Uniform distribution around the circumference therefore results in an angular spacing of $\varphi = 2\pi/(m-1)$, which, as may be seen from equation (34), gives a singular matrix.

In summary, if the m measurements are uniformly distributed around the circumference the angular spacing is $\varphi = 2\pi/m$ which makes the matrix $\mathbf{T}$, in general, non-singular. If one of those measurements is taken at the centre of the circle and the remaining $(m-1)$ uniformly distributed around the circumference, the angular spacing is $\varphi = 2\pi/(m-1)$, and the resulting matrix is always singular.

The Fourier coefficients may also be estimated solely from measurements of surface strain. The surface strain in the radial direction is given by

$$\varepsilon_r = -\frac{h}{2}\frac{\partial^2 w}{\partial \hat{r}^2} \tag{37}$$

where h is the thickness of the plate. Substituting the expression for displacement given in equation (29) into equation (37) and differentiating to yield an expression for radial strain in terms of the Fourier series coefficients gives

$$\epsilon_r \approx \frac{hk_p^2}{2}\sum_{h=-q}^{q} C_n\, \mathrm{e}^{\mathrm{i}n\phi}\int_{-\pi}^{\pi} \cos^2\theta\, \mathrm{e}^{\mathrm{i}n\theta}\, \mathrm{e}^{-\mathrm{i}k_pR\cos\theta}\, \mathrm{d}\theta. \tag{38}$$

If the strain gauges are placed with a uniform angular spacing, φ, on the circumference of a circle of radius R, as shown in Figure 1, it can be shown from equation (38) that the elements of the transformation matrix, $\mathbf{T}$, are given by

$$\mathbf{T}_{j,\,s_n} = \frac{hk_p^2}{2}\,\mathrm{e}^{\mathrm{i}n(j-1)\varphi}\int_{-\pi}^{\pi} \cos^2\theta\, \mathrm{e}^{\mathrm{i}n\theta}\, \mathrm{e}^{-\mathrm{i}k_pR\cos\theta}\, \mathrm{d}\theta = \mathrm{e}^{\mathrm{i}n(j-1)\varphi}V_n, \tag{39}$$

where

$$V_n = \frac{hk_p^2}{2}\int_{-\pi}^{\pi} \cos^2\theta \mathrm{e}^{\mathrm{i}n\theta}\,\theta\, \mathrm{e}^{-\mathrm{i}kR\cos\theta}\, \mathrm{d}\theta = -\frac{\pi hk_p^2}{4}(-\mathrm{i})^n(\mathrm{J}_{n-2}(k_pR) - 2\mathrm{J}_n(k_pR) + \mathrm{J}_{n+2}(k_pR)) \tag{40}$$

and s_n is the column of matrix, $\mathbf{T}$, associated with Fourier index n. The similarity to the case in which displacement was measured is readily apparent. Since V_n is constant for any given column, the zeroes of the determinant of matrix, $\mathbf{T}$, are the same as those of the auxiliary matrix, $\bar{\mathbf{T}}$, obtained by dividing each column of $\mathbf{T}$ by the appropriate V_n. This auxiliary matrix is precisely the same as that determined for the displacement measurements. All of the preceding comments regarding the angular spacing of displacement measurements and singularity are therefore equally valid for measurements of radial strain.

Matrix singularity will also occur if one of the values of U_n (or V_n for strain measurements) is zero, since this will result in the elements of a column of the matrix, $\mathbf{T}$, being identically zero. As U_n and V_n are functions of the Fourier index, n, and the radius of the circle (in radians) upon which the transducers are placed, k_pR (that is, the radius of the circle non-dimensionalized with respect to plate wavenumber, and hereafter referred to as the tranducer placing radius), they have roots at specific combinations of these variables. It is therefore necessary to avoid such placing radii for all the Fourier coefficients

TABLE 1

Transducer placing radii (k_pR) resulting in matrix singularity

Fourier index, n	Roots of U_n (displacement or acceleration)	Roots of V_n (strain)
0	$k_pR = 2{\cdot}40$	$k_pR = 1{\cdot}84$
± 1	$k_pR = 3{\cdot}84$	$k_pR = 3{\cdot}52$
± 2	$k_pR = 5{\cdot}14$	$k_pR = 1{\cdot}56$
± 3	$k_pR = 6{\cdot}39$	$k_pR = 2{\cdot}65$

being evaluated. Non-zero transducer placing radii that result in zeroes of U_n and V_n, and hence singularity of matrix **T**, when evaluating low order Fourier coefficients from displacement and strain measurements are shown in Table 1. Physically, these radii may be interpreted as locations at which a particular Fourier coefficient makes no contribution to the measured variable. This is readily understood when considering the measurement of displacement. Each Fourier coefficient represents a reverberant wave field, since the magnitude of the assumed wave remains constant with changing direction—only the phase varies. If that wave field were present in isolation, then there would be nodes at which there was no motion. The roots of U_n correspond to nodes of the assumed wave field, and thus if measurements are taken at those points then that particular Fourier coefficient cannot be determined.

While the use of identical transducers uniformly distributed on the circumference of a circle will allow the required Fourier coefficients to be estimated if specific placing radii are avoided, there are other options. These include: (i) the use of an overdetermined system, in which the number of measurements exceeds the number of Fourier coefficients being estimated, utilizing the Moore–Penrose inverse; (ii) the use of transducer arrays with a non-uniform angular spacing; and (iii) modification of the matrix, **T**, by equating the very small singular values and their corresponding elements in its inverse to zero, as proposed by Nash [17].

While the use of an overdetermined system does increase flexibility in transducer placing, it means that additional transducers and measurement channels are required, increasing the cost of the measurement system. If near singularity cannot be avoided, the modification of matrix, **T**, which improves conditioning at the expense of theoretical accuracy, appears to hold some promise. However, while such mathematical techniques for dealing with ill-conditioned problems exist, it is preferable to work with a well-conditioned problem if possible.

6. CONDITIONING

As stated in section 1, the conditioning of a problem is a measure of the sensitivity of the final result to errors in the input data. In the calculation of structural intensity, this is determined both by the measurement system used and the vibrational field present. It is possible, however, to isolate the two effects and thus to compare different measurement systems in terms of the conditioning offered. The calculation of the intensity using equations (23) and (24) is determined, to within a constant factor, by the values of the Fourier coefficients. Owing to the assumptions and approximations used, the measurement system will have some influence on the values of these coefficients, but they are essentially descriptors of the vibrational field. The conditioning of equations (23) and (24) is therefore primarily determined by the nature of the vibration. In contrast, the evaluation of the Fourier coefficients from measured variables as described in section 5 involves solving a

set of simultaneous equations. These may be written in matrix form and the conditioning judged using the two-norm condition number of the matrix. The matrix is determined by the parameters being measured, the measurement locations and the number of coefficients being evaluated, and may be considered a property of the measurement system.

While the condition number of the transformation matrix provides an indication of conditioning, this may not be sufficient for the comparison of dissimilar measurement systems. It is governed not only by the choice of measured variables and measurement spacing, but also by the chosen co-ordinate origin and the relative magnitude of each row of the matrix. The centre of the measurement array has already been designated as the co-ordinate origin for mathematical simplicity, eliminating this source of variation, but for comparative purposes the normalizing of the matrix rows through division by the constant (i.e., not θ dependent) terms associated with each row, is proposed. The two-norm condition number of this modified matrix is directly analogous to the array condition number proposed for the comparison of intensity measurement systems on beams [13]. With this standardization, different transducer arrays can be compared in terms of their sensitivity to measurement error. However, in view of the practical difficulties in obtaining accurate phase matching between dissimilar transducer types, only arrays involving one transducer type will be considered in this paper. Normalization is therefore unnecessary, and we are simply interested in the two-norm condition number of matrix **T**.

For a transducer system giving m measurements of displacement, at radius R and uniform angular spacing $\varphi = 2\pi/m$, the elements of matrix **T** are given by equation (30) as

$$\mathbf{T}_{j,\,s_n} = \mathrm{e}^{[\mathrm{i}2n\pi(j-1)]/m} U_n. \tag{41}$$

Since U_n is constant for a particular n, the magnitudes of the elements in any given column, s_n, are equal. Furthermore, if each column is normalized to have a magnitude of one by dividing by the appropriate $|U_n|$, then the resulting matrix has a condition number of unity. The columns (and rows) of this matrix are therefore orthogonal. As the matrix, **T**, may be found from this normalized matrix by multiplying each column by the appropriate $|U_n|$, the condition number of **T** is given by the ratio of the largest and smallest $|U_n|$, being

$$\alpha_a = |U_n|_{max}/|U_n|_{min}. \tag{42}$$

It is clear that as the magnitude of Fourier index, n, becomes large,

$$U_n = \int_{-\pi}^{\pi} \mathrm{e}^{\mathrm{i}n\theta}\, \mathrm{e}^{-\mathrm{i}k_pR\cos\theta}\, \mathrm{d}\theta \rightarrow \int_{-\pi}^{\pi} \mathrm{e}^{\mathrm{i}n\theta}\, \mathrm{d}\theta = 0, \tag{43}$$

since the $\mathrm{e}^{\mathrm{i}n\theta}$ term dominates $\mathrm{e}^{-\mathrm{i}k_pR\cos\theta}$ over most of the range of integration, particularly if the tranducer placing radius, k_pR, is small. This can also be seen from the asymptotic expansion of the Bessel function for large positive real orders [15],

$$\mathrm{J}_n(k_pR) \sim \frac{1}{\sqrt{2\pi n}} \left(\frac{ek_pR}{2n}\right)^n, \tag{44}$$

which decreases in proportion to $(1/n)^{n+0{\cdot}5}$. For typical values of k_pR in the range of 0·5–1·5, the maximum $|U_n|$ occurs for $n = 0$ or $n = \pm 1$. Subsequent increases in $|n|$ cause a decrease in $|U_n|$, the rate of decrease being faster for smaller values of k_pR. In view of the previous comments relating $|U_n|$ to the condition number it is apparent that conditioning deteriorates as more Fourier coefficients are estimated or, for typical spacings, as the transducer spacing is reduced. This is readily understood in physical terms

by considering the influence that each Fourier coefficient has on the individual measurements. The conditioning is, in essence, a measure of the relative importance of the individual coefficients in the Fourier series expansions of the measured variables. Good conditioning indicates that all the coefficients make a significant contribution to the expansions, while poor conditioning occurs if one or more coefficients are insignificant in the expansions. If acceleration is measured at points on a circle centred on the co-ordinate origin and the radius of that circle is very small, then the Fourier series expansions of those measurements will be dominated by the C_0 coefficient. This is because the displacement, and hence the acceleration, at the origin is completely defined by C_0. The Fourier series expansions of the measurements therefore converge rapidly, the higher order terms making little contribution, and the conditioning is poor. As the transducer placing radius is increased the higher order terms make a larger contribution to the Fourier series expansions of the measurements, which thus converge more slowly, and conditioning improves up to a point. Increasing the radius beyond this point causes the condition to deteriorate owing to the reducing influence of C_0. In practical situations, however, transducer placing radii would be relatively small, and under these circumstances improved conditioning occurs in conjunction with slower convergence of the Fourier series expansions.

Similar comments apply to intensity estimates from the measurement of radial strain. For a transducer system giving m measurements of radial strain at radius R and uniform angular spacing $\varphi = 2\pi/m$, the elements of matrix $\mathbf{T}$ are given by equation (39) as

$$\mathbf{T}_{j,\,s_n} = \mathrm{e}^{[\mathrm{i}2n\pi(j-1)]/m} V_n . \tag{45}$$

The condition number of the transformation matrix, $\mathbf{T}$, is given by the ratio of the magnitudes of the largest and smallest V_n, being

$$\alpha_s = |V_n|_{max} / |V_n|_{min} . \tag{46}$$

These characteristics are identical to those inherent with the accelerometer array: however, the rate at which $|V_n|$ decreases with increasing n and decreasing $k_p R$ is substantially lower than the rate of decrease of $|U_n|$. This means that, for a given small transducer placing radius, $k_p R$, the conditioning offered by strain measurement can be significantly better than that offered by displacement or acceleration measurement.

7. SYSTEMATIC ERRORS

The systematic errors that arise from the use of a particular arrangement of transducers and method of processing are the result of the discrepancy (if any) between the true and assumed deformations. This discrepancy may be due to assumptions regarding the vibrational field (e.g., that far field conditions exist, or that only plane propagating waves are present) or to approximations that are made to simplify measurements and processing (e.g., that spatial derivatives of displacement may be determined using simple finite difference approximations and thus the deformation has a low order polynomial form, or that the higher order terms in the Fourier series expression for wave amplitude may be ignored when the coefficients are evaluated). The effects of these assumptions and approximations, and therefore also the resultant systematic errors, are thus dependent on the specific field conditions.

In this section the systematic errors that result from the use of the Fourier series approach to plate intensity measurement are discussed. Two simple cases are studied numerically: intensity measurement in the presence of a plane propagating wave and intensity measurement in the vicinity of a point source. The former simulation illustrates

the effect of truncating the Fourier series, since the field conditions match the assumption of plane wave propagation. In the latter simulation the assumption of plane wave propagation is violated owing to the presence of near field waves and of propagating waves that exhibit geometrical decay due to curvature of the wavefront. It thus gives an indication of the sensitivity of the measurement technique to these characteristics.

7.1. SYSTEMATIC ERRORS IN THE PRESENCE OF PLANE PROPAGATING WAVES

The Fourier series approach to intensity measurement, as described in this paper, is based on the assumption that the wave field is composed purely of plane propagating waves. Under these conditions it would give an exact result if an infinite number of coefficients were evaluated. However, as it is only possible to evaluate a finite number of coefficients, a systematic error is introduced. When certain Fourier coefficients are ignored, as they are when only m terms are found, those coefficients that *are* evaluated must deviate from their true values in compensation. If the Fourier series expansions of the measured variables converge rapidly, then the higher order coefficients are small, and their truncation has a relatively small effect on the values of the calculated coefficients. If, however, the expansions converge slowly the higher order coefficients are large, and the effects of truncation large also. Since, for typical transducer placing radii, improved conditioning and slower convergence of the Fourier series expansions both result from increasing the placing radius, reduced systematic errors are achieved at the expense of conditioning.

In practice, the error that results from truncating the Fourier series appears predominantly to affect the highest order coefficient evaluated. It is therefore advantageous to evaluate more than the five coefficients necessary to calculate the intensity. The error is then largely restricted to coefficients that have no direct influence on the intensity estimate. This is apparent from Table 2, in which are given the coefficients for a wave of unit amplitude propagating in the x-direction, calculated from five, seven and nine acceleration measurements. The true values of the coefficients are given by

$$\begin{aligned} C_n &= \frac{1}{2\pi}\int_{-\pi}^{\pi} A(\theta)\,\mathrm{e}^{-\mathrm{i}n\theta}\,\mathrm{d}\theta \\ &= \frac{1}{2\pi}\int_{-\pi}^{\pi} \delta(\theta)\,\mathrm{e}^{-\mathrm{i}n\theta}\,\mathrm{d}\theta \\ &= 0{\cdot}1592, \ldots, \qquad n = 0, \pm 1, \pm 2, \ldots . \end{aligned} \tag{47}$$

It can be seen that the evaluation of a larger number of coefficients reduces the error in the coefficients, C_{-2}–C_2, used to calculate the intensity: however, this results in poorer conditioning, more expensive measurement systems and greater computational requirements. A measurement system in which seven Fourier coefficients are estimated therefore seems appropriate, although, depending on the accuracy required, satisfactory results may be achieved with the evaluation of five coefficients.

The effects of truncation of the Fourier series on the intensity estimate can be seen by simulating the incidence of a plane propagating wave on the transducer array. In the light of the foregoing discussion, measurements of acceleration at seven locations, with a uniform angular spacing on the circumference of a circle, have been simulated and used to determine seven Fourier coefficients. The intensity has then estimated from these coefficients as described in section 4. For comparative purposes, the intensity has also estimated using a finite difference based approach suitable for far field conditions. Spatial derivatives of up to second order have been estimated from simulated measurements of

TABLE 2

Fourier coefficients evaluated for a plane wave of unit amplitude propagating in the x-direction, using five, seven and nine accelerometers

Placing radius:	$k_pR = 0{\cdot}1$			$k_pR = 0{\cdot}5$			$k_pR = 1$			$k_pR = 2$		
Number of accelerometers	5	7	9	5	7	9	5	7	9	5	7	9
Condition numbers	799	47 910	$3{\cdot}83 \times 10^6$	30·7	366	5838	6·66	39·1	309	2·58	4·47	16·96
C_{-4}	—	—	0·1592−	—	—	0·1591−	—	—	0·1592−	—	—	0·1592−
	—	—	0·0016i	—	—	0·0080i	—	—	0·0161i	—	—	0·0330i
C_{-3}	—	0·1592−	0·1592	—	0·1592−	0·1592	—	0·1592−	0·1592+	—	0·1592−	0·1592+
	—	0·0020i	—	—	0·0100i	—	—	0·0201i	0·0002i	—	0·0420i	0·0015i
C_{-2}	0·1592−	0·1592	0·1592	0·1592−	0·1592	0·1592	0·1592−	0·1592+	0·1592	0·1591−	0·1592+	0·1592−
	0·0027i	—	—	0·0133i	—	—	0·0271i	0·0003i	—	0·0582i	0·0032i	0·0001i
C_{-1}	0·1592	0·1592	0·1592	0·1592+	0·1592	0·1592	0·1592+	0·1592	0·1592	0·1592+	0·1592−	0·1592
	—	—	—	0·0001i	—	—	0·0009i	—	—	0·0090i	0·0003i	—
C_0	0·1592	0·1592	0·1592	0·1592	0·1592	0·1592	0·1592−	0·1592	0·1592	0·1592−	0·1592+	0·1592
	—	—	—	—	—	—	0·0001i	—	—	0·0100i	0·0002i	—
C_1	0·1592	0·1592	0·1592	0·1592+	0·1592	0·1592	0·1592+	0·1592	0·1592	0·1592+	0·1592−	0·1592
	—	—	—	0·0001i	—	—	0·0009i	—	—	0·0090i	0·0003i	—
C_2	0·1592−	0·1592	0·1592	0·1592+	0·1592	0·1592	0·1592−	0·1592+	0·1592	0·1591−	0·1592+	0·1592−
	0·0027i	—	—	0·0133i	—	—	0·0271i	0·0003i	—	0·0582i	0·0032i	0·0001i
C_3	—	0·1592−	0·1592	—	0·1592−	0·1592	—	0·1592−	0·1592+	—	0·1592−	0·1592+
	—	0·0020i	—	—	0·0100i	—	—	0·0201i	0·0002i	—	0·0420i	0·0015i
C_4	—	—	0·1592−	—	—	0·1591−	—	—	0·1592−	—	—	0·1592−
	—	—	0·0016i	—	—	0·0080i	—	—	0·0161i	—	—	0·0330i

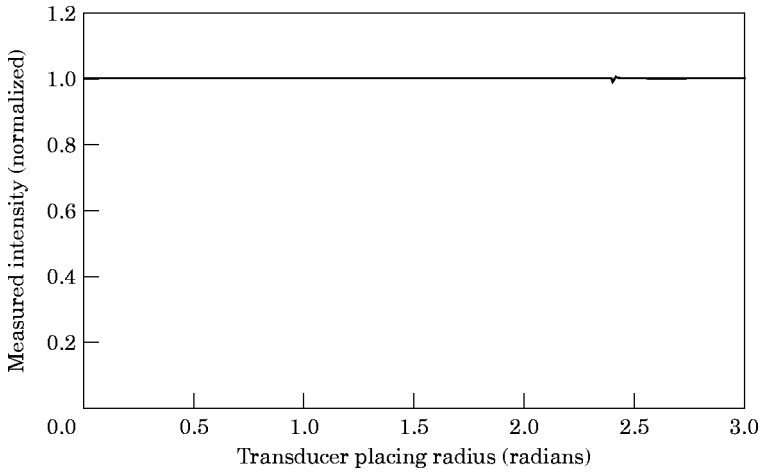

Figure 2. The systematic error in the Fourier series approach using seven accelerometers in the presence of one-dimensional wave propagation. ——, $\theta = 0$; -----, $\theta = 0{\cdot}15\pi$; ·····, $\theta = 0{\cdot}3\pi$; –·–·–·–, $\theta = 0{\cdot}45\pi$.

acceleration at nine locations [10], as described in Appendix 1, and substituted in equations (19) and (20) to calculate the intensity.

A complication arising from this comparison is the different transducer arrangements required. The Fourier series approach uses accelerometers arranged in a circle, while they are placed in a square for the finite difference approach. The term "transducer placing radius" ($=k_pR$) is therefore used to describe the size of the Fourier series array, and "transducer separation" ($=k_p\Delta$) to describe that of the finite difference approach. While the terminology differs, when these measures are equal the overall size of the arrays, and the distances between adjacent accelerometers, are very similar.

The component of intensity in the x-direction measured using the Fourier series approach is shown (normalized with respect to the true intensity in the x-direction) as a function of transducer placing radius in Figure 2 for four propagation directions, the lines being overlaid. It is apparent that the systematic errors are very low almost irrespective of transducer placing radius and propagation direction. The small irregularity visible at a transducer placing radius of $k_pR = 2{\cdot}4$ is due to near singularity of the transformation matrix, **T**, as predicted in Table 1.

The intensity measured using the finite difference approach, again normalized with respect to the true intensity, is shown in Figure 3. The systematic error in this case is significantly influenced by both the transducer spacing and the propagation direction. Large non-dimensionalized transducer spacings result in large relative errors, these being greatest when the propagation direction, and hence also the direction of energy flow, coincides with the x-axis, giving large absolute errors.

7.2. SYSTEMATIC ERRORS IN THE VICINITY OF A POINT SOURCE

While the plane wave propagation assumed in the Fourier series approach is possible in a plate, it is not the only solution to the equation of motion, even in the far field. The derivation in section 2 leading to this assumption was based not only on the region being remote from discontinuities (so that the effects of near fields are negligible), but also on the extent of that region being small relative to the distance from all discontinuities and sources of excitation (to minimize the effects of geometrical decay). Under other conditions different wave types may exist, violating the assumption of only plane propagating waves being present and thus introducing a further systematic error.

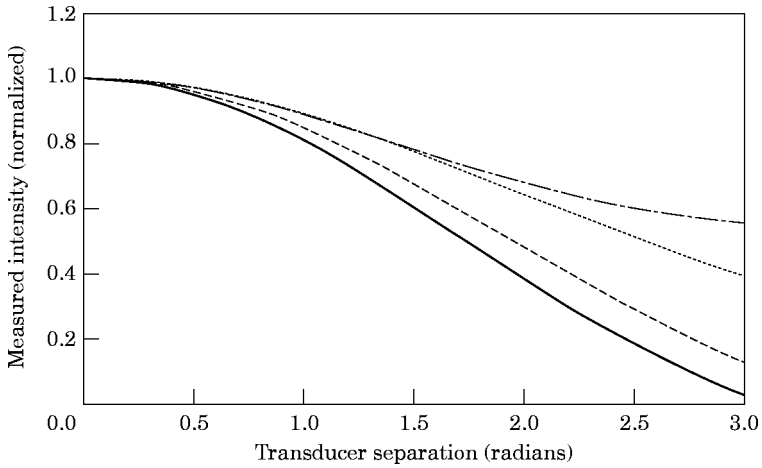

Figure 3. The systematic error in finite difference approach using nine accelerometers in the presence of one-dimensional wave propagation. ——, $\theta = 0$; -----, $\theta = 0{\cdot}15\pi$; ·····, $\theta = 0{\cdot}3\pi$; –·–·–·–, $\theta = 0{\cdot}45\pi$.

To illustrate this effect, the Fourier series and finite difference approaches described in the previous subsection have been used in the simulation of intensity measurements in the vicinity of a point source. The displacement for this excitation is given by equation (3) and, as stated in section 2, includes both near fields and non-planar propagating waves. It is assumed that both the source and the centre of the transducer array lie on the x-axis. The calculated intensity in the x-direction (normalized with respect to its true value) is shown as a function of the distance between the source and the array centre in Figures 4 and 5 for the Fourier series and finite difference approaches respectively.

It is apparent that both approaches result in the intensity being underestimated in measurements close to the source. However, the errors and the influence of the transducer spacing on these measurements are larger in the finite difference approach than in the Fourier series approach. At large distances from the source the systematic error in the two approaches is similar to that for plane wave propagation. Under these circumstances the error in the Fourier series approach is small almost irrespective of the transducer placing

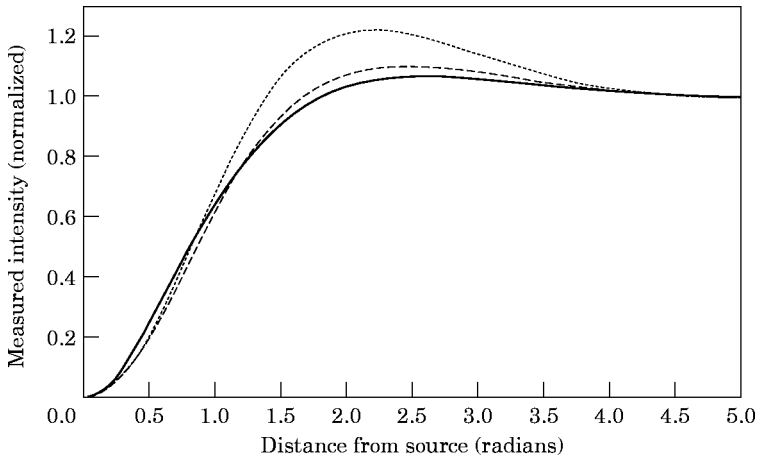

Figure 4. The systematic error in Fourier series approach in vicinity of a point source. ——, $k_pR = 0{\cdot}5$; -----, $k_pr = 1$; ·····, $k_pR = 1{\cdot}5$.

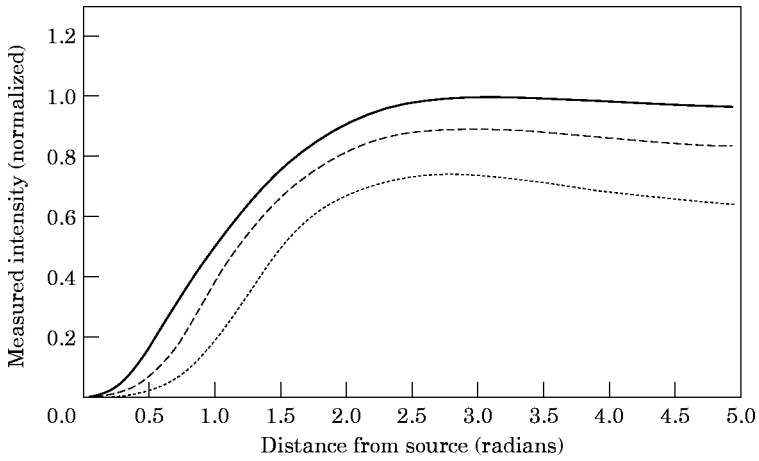

Figure 5. The systematic error in finite difference approach in vicinity of a point source. ——, $k_p\Delta = 0{\cdot}5$; -----, $k_p\Delta = 1$; ·····, $k_p\Delta = 1{\cdot}5$.

radius, while the finite difference approach results in an underestimation that increases with increasing transducer spacing. At intermediate distances from the source the error in both approaches is dependent on the transducer spacing. It can be seen, however, that the errors of the Fourier series approach are generally smaller than those of the finite difference approach when similarly sized transducer arrays are used.

8. RANDOM ERRORS

With perfect knowledge of the measured variables and the relevant properties of the plate, it would only be necessary to consider systematic errors. In reality, however, there is a degree of uncertainty in our knowledge of these parameters, and this uncertainty introduces random errors into the intensity estimate. The degree to which errors in the input data affect the result of the intensity calculation is governed by the conditioning of the problem. As stated in section 6, this is determined by both the vibrational field present and the particular measurement system and processing used.

To illustrate the effects of errors in the input data, numerical simulations have been performed, assuming that plane waves of amplitude 1 and 0·4 are propagating in the positive and negative x-directions respectively. The responses at the relevant locations have been calculated, and random errors then applied to various input parameters. The intensity was then calculated using the Fourier series and finite difference approaches described in the previous section. The following graphs show the normalized difference between this measurement and the intensity calculated in the absence of errors in the input parameters.

In Figures 6 and 7 are shown the errors that occur when using the Fourier series and finite difference approaches if the measured variables are subjected to random phase errors uniformly distributed on the interval $[-2^\circ, +2^\circ]$. Both approaches show a high sensitivity to phase error at small non-dimensional transducer spacings, which decreases as the spacing increases. The sensitivity of the Fourier series approach also becomes large at a transducer placing radius of $k_pR \approx 2{\cdot}4$, this coinciding with the condition of the transformation matrix, **T**, deteriorating and approaching singularity. The pronounced minimum in the sensitivity of the finite difference approach at a quarter-wavelength spacing is a result of there being an optimal $\pi/2$ phase difference between adjacent

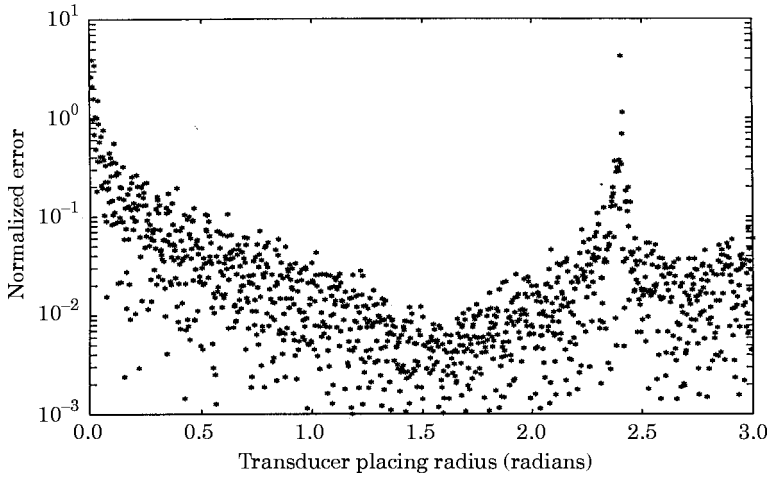

Figure 6. The effect of random phase errors on the intensity estimate: Fourier series approach.

measurements in the x-direction under these circumstances, and is not typical of other propagation directions.

In Figures 8 and 9 are shown the errors in the intensity estimate if random errors, uniformly distributed on the interval $[-2\%, +2\%]$, are applied to the magnitude of the measured variables. Small spacings result in a high sensitivity to this error for both approaches, the sensitivity reducing with increasing transducer separation. The sensitivity of the Fourier series approach again becomes large as the condition of the transformation matrix deteriorates and nears singularity.

The sensitivity to amplitude and phase errors also gives an indication of sensitivity to errors in transducer placement. If a transducer is displaced by a small amount, then the measured variable will change. The size of this change will depend on the field conditions, but the effect on the intensity estimate will be determined by the sensitivity of the calculation to changes in the measured variable.

The effect of a random variation in the wavenumber, uniformly distributed on the interval $[-2\%, +2\%]$, on the Fourier series and finite difference approaches is shown in

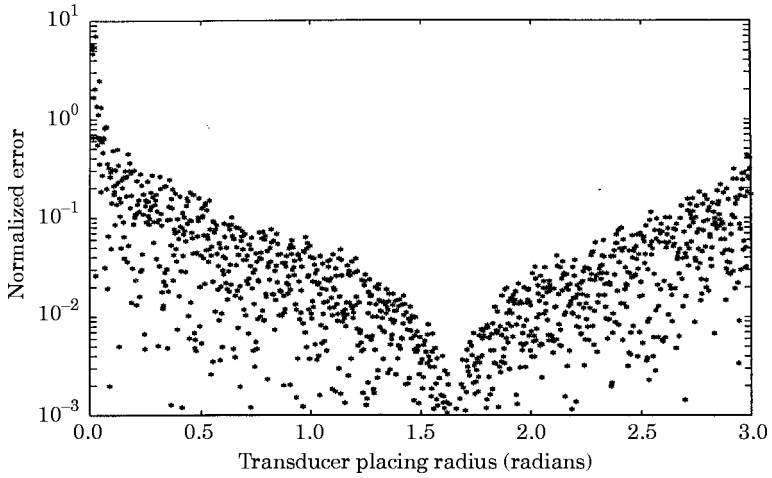

Figure 7. The effect of random phase errors on the intensity estimate: nine-point finite difference approach.

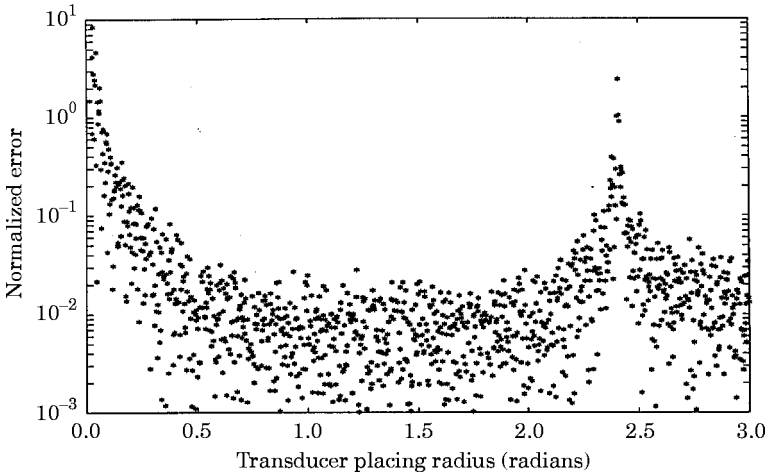

Figure 8. The effect of random amplitude errors on the intensity estimate: Fourier series approach.

Figures 10 and 11 respectively. The sensitivity of the Fourier series approach to this error increases with increasing transducer placing radius, reaching a maximum at $k_p R \approx 2{\cdot}4$ when the transformation matrix, **T**, is singular. It is also consistently higher than that of the finite difference approach, which is almost independent of transducer spacing. The greater sensitivity of the Fourier series approach may be explained by the use of the wavenumber both in the evaluation of the Fourier coefficients and as a factor to the third power in the entire intensity expression. In contrast, it is only used as a factor to the second power in the estimation of the shear component of intensity in the finite difference approach.

9. EXPERIMENTAL INTENSITY MEASUREMENT

A brass plate, $1800 \times 850 \times 3$ mm, was mounted to approximate simple supports on three boundaries with the fourth (short) edge free. Damping, in the form of sand and felt, was applied in the region of the free edge. The use of simple supports meant that, in regions

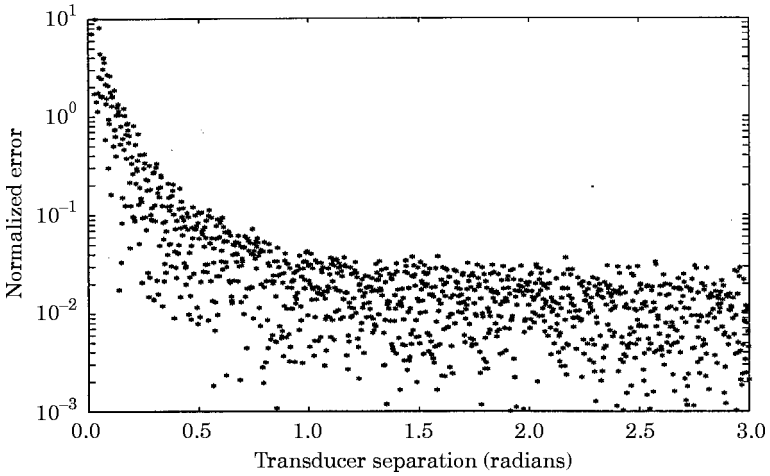

Figure 9. The effect of random amplitude errors on the intensity estimate: nine-point finite difference approach.

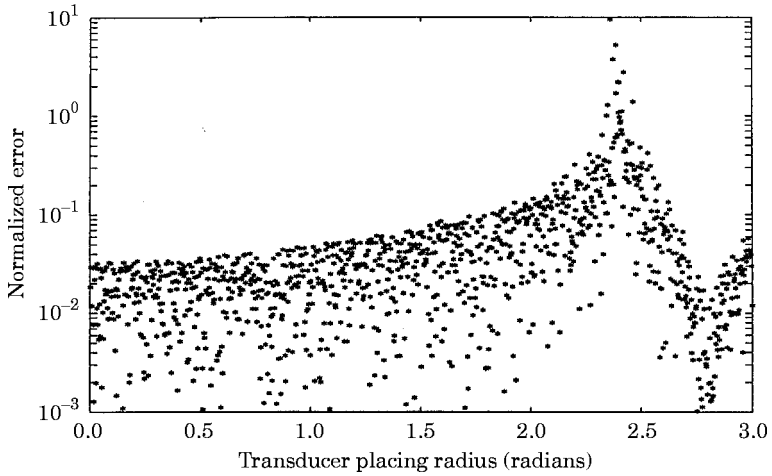

Figure 10. The effect of random errors in wavenumber estimate: Fourier series approach.

sufficiently distant from the excitation point and damping, the effects of near fields at the plate boundary could be ignored, permitting the use of a far field intensity measurement system close to the edges of the plate. The driving point accelerance was measured using a Hewlett Packard HP35665A Dynamic Signal Analyzer, and the natural frequencies and damping ratios for the plate, in damped and undamped form, estimated using in-built functions of the analyzer. Measurements on the damped plate showed typical loss factors of 2–3% in the frequency range 100–500 Hz, these being typically a factor 20–40 times greater than the loss factors in the undamped plate. The exceptions to this occurred at around 260 Hz and 460 Hz, where the damping was ineffective, giving loss factors $\sim 0{\cdot}2\%$. To a good approximation, however, the energy supplied to the plate may be considered dissipated solely in the damped region, and the energy flow down the plate should be equal to the power input.

The plate was excited using a rapid sine sweep through the frequency range of interest, with the duration of the sweep being selected to ensure that the full response of the plate was captured in the measurement. Power input to the plate was determined from the driving force (using a Brüel and Kjær Type 8200 force transducer and Type 2635 charge

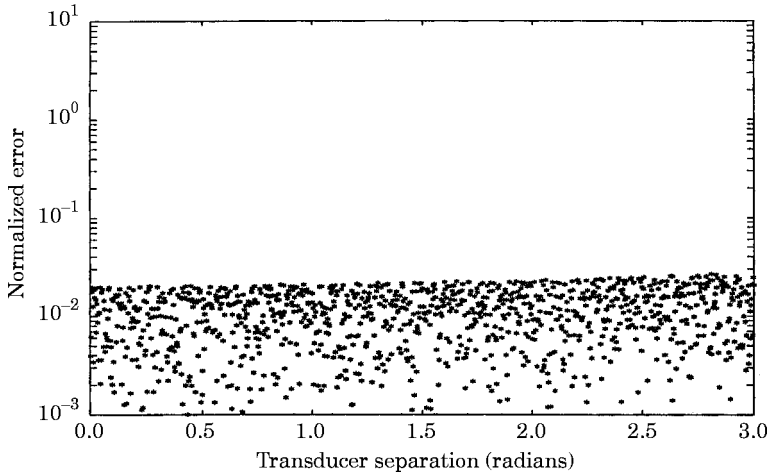

Figure 11. The effect of random errors in the wavenumber estimate: nine-point finite difference approach.

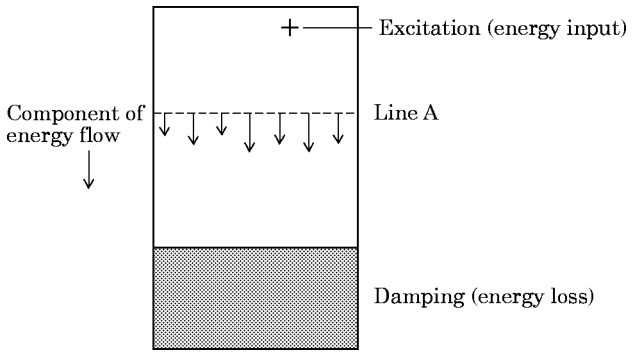

Figure 12. A schematic diagram of the experimental set-up.

amplifier) and driving point acceleration (using a PCB 321 A03 accelerometer), while the intensity was estimated using seven PCB 353B65 accelerometers. All signals were low-pass filtered using an Onsite Instruments TF16 16-channel filter, with data acquisition and processing performed using an IBM Pentium 90 PC equipped with a National Instruments AT-MIO-16L-9 Multifunction I/O board. LabVIEW software was used to control the data acquisition as well as for subsequent processing. The experimental apparatus and procedure are described in more detail in reference [18].

For each intensity measurement, seven acceleration measurements were taken at a uniform angular spacing on a circle of 50 mm radius, this being approximately a tenth of a wavelength at 100 Hz and a quarter-wavelength at 500 Hz, and used to estimate seven Fourier coefficients. The intensity at a point was calculated as the average of three individual intensity measurements, and determined at 31 points, 25 mm apart, on a line across the plate (see Figure 12). The net energy flow across this line was estimated from the intensity at these points.

Power input to the plate and the net energy flow as measured using the Fourier series approach are shown in Figure 13, and the relative difference between the two measurements in Figure 14. It is apparent that the input power and measured energy flow are generally in good agreement, with the greatest differences occurring at approximately 260 and 460 Hz. The damping at these frequencies was relatively low, as noted earlier, with loss factors of $\sim 0{\cdot}2\%$, and it is believed that the discrepancies are probably due to phase

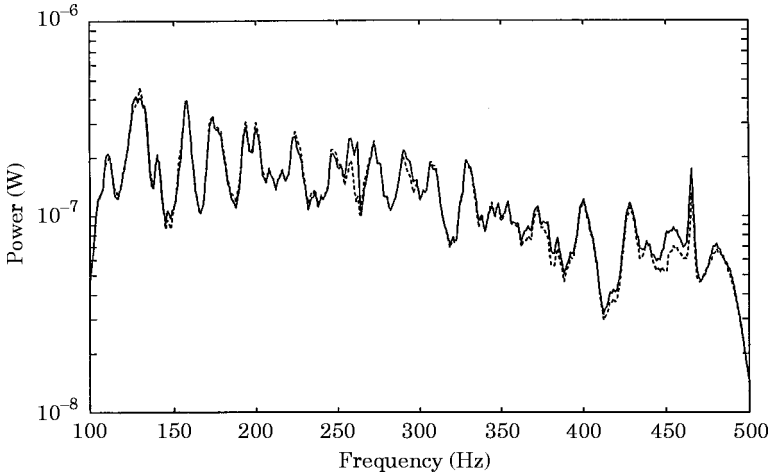

Figure 13. The input power and the measured energy flow in a plate: ——, Input power; ---, energy flow.

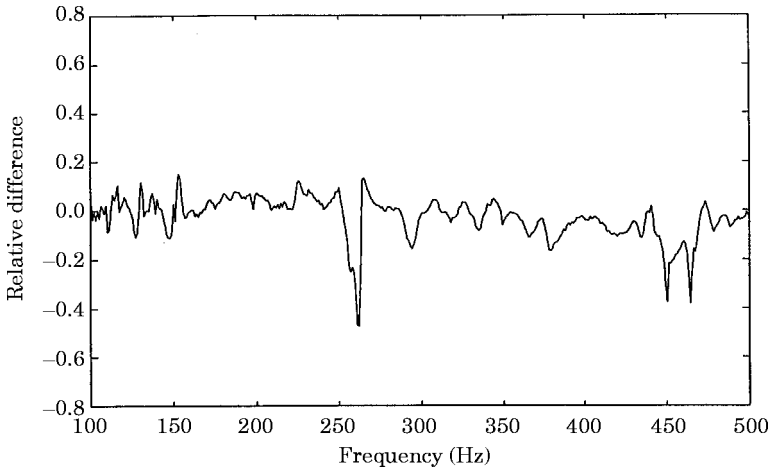

Figure 14. The relative difference between the measured power input and the energy flow, measured using the Fourier series approach.

mismatch between channels, to which intensity measurements are extremely sensitive in highly reverberant fields.

10. CONCLUDING REMARKS

As there does not exist a general closed form solution for the motion of a vibrating plate, any attempt to determine the structural intensity in a plate from a finite number of measurements will result in a systematic error. This error is the result of a discrepancy between the true and assumed deformations, and the requirements for minimizing it will, for a particular measurement system, conflict with the requirements for a well-conditioned problem. It is thus desirable to find an optimum compromise between systematic and random errors. This can be achieved through the use of appropriate functions to interpolate between the measurement points in the transducer array. If these interpolating functions, and thus the assumed deformation, closely approximate the plate deformation then the systematic errors will be small, regardless of the separation of the measurement points, and this separation can then be chosen almost purely on the basis of achieving a well-conditioned problem. The fact that, in a region sufficiently remote from discontinuities and excitation, the vibrational field in a plate approximates plane wave propagation makes this form of displacement a logical assumption for far field intensity measurements on plates.

In the Fourier series approach to intensity measurement, as described in this paper, it is assumed that, within a region, the motion of the plate can be approximated as the sum of plane propagating waves, and that the wave amplitude is a function of the propagation direction. This function is written as a complex Fourier series, which is truncated to allow the Fourier coefficients to be estimated from a finite number of measurements. The intensity can be expressed in terms of the Fourier coefficients, with only the five coefficients of lowest order contributing to the intensity at the co-ordinate origin owing to the orthogonality of trigonometric functions. The truncation of the Fourier series introduces a systematic error which, for typical transducer placing radii, increases as the conditioning improves and so results in the expected compromise between systematic and random errors. However, this truncation predominantly affects the highest order coefficient, and thus by evaluating more than the required five coefficients the effects of truncation can be minimized.

The Fourier coefficients are estimated by solving a set of simultaneous equations relating to the measured variables. These equations can be written in matrix form, and thus the conditioning of the problem can be judged in terms of the two-norm condition number of a matrix, as previously proposed for beam intensity measurements [13]. Measurement systems involving transducers placed at a uniform angular spacing on the circumference of a circle have been shown to be suitable for determining the coefficients.

The effects of material damping may be incorporated into this approach through the use of a complex elastic modulus, E, and a consequent complex plate wavenumber, k_p. This has an influence both on the expressions for intensity in terms of the Fourier coefficients and on the manner in which the Fourier coefficients are estimated. The presence of material damping changes the phase relationship between displacement and its various spatial derivatives, and hence also between the various forces and velocities used to estimate the intensity. However, provided that the damping is light, the effect on the total intensity is small, and the assumption of a purely real wavenumber is justifiable. A similar approach is also warranted in the estimation of the Fourier coefficients when damping is light. It is necessary for the attenuation due to damping of a wave as it propagates from one side of the transducer array to the other to be measurable if the use of a complex wavenumber is to be worthwhile. If a transducer placing radius, $k_pR = 1{\cdot}5$, and a loss factor of 1% are assumed to be typical, the wave amplitude will be attenuated by approximately 1% in travelling across the array. In reality, this level of accuracy will be difficult to achieve, and the use of a complex wavenumber in the estimation of the Fourier coefficients is probably only worthwhile if the material damping is relatively strong.

Numerical simulations have been performed to compare a Fourier series intensity measurement in which seven coefficients are evaluated to a finite difference approach using nine measurement points. These have shown the Fourier series approach to have low levels of systematic error in the presence of plane waves, almost irrespective of transducer placing radius and wave propagation direction. In contrast, the finite difference approach exhibits large systematic errors, which are dependent on the propagation direction, if a large transducer separation is used. In the vicinity of a point source, where the assumption of plane wave propagation is violated and therefore where the systematic errors could be expected to be large, the systematic error of the Fourier series approach was generally lower than that of the finite difference approach with a similar overall transducer array size. For typical transducer spacings the effects of the near field and non-planar propagating waves on the two approaches become relatively small at distances greater than a half-wavelength from the source, and at large distances the systematic errors asymptotically approach those found in the presence of a plane propagating wave.

A comparison of these Fourier series and finite difference approaches using similar overall transducer array sizes in a specific vibrational field showed them to be similar in terms of sensitivity to errors in the magnitude and phase of the measured variables. However, the sensitivity of the Fourier series approach to errors in the wavenumber estimate was seen to be greater than that of the finite difference approach. This is a consequence of the greater importance of the wavenumber in the Fourier series approach, it being used both in the estimation of the Fourier coefficients and as a factor to the third power in the entire intensity expression. In contrast, the wavenumber is only involved as a factor to the second power in the estimation of the shear component of intensity, and not at all for the bending and twisting moment components, in the finite difference approach used.

These sensitivities, while specific to the particular vibrational field assumed, illustrate how a small transducer spacing results in a high sensitivity to errors in the measured variables. However, the low systematic error of the Fourier series approach allows

relatively large transducer placing radii to be used. This is in contrast to the finite difference approach, where the large systematic errors at large transducer separations mean that the spacing should ideally be relatively small. As a consequence, the Fourier series approach would appear to offer a potentially better compromise between systematic errors and sensitivity to errors in the measured variables. This is achieved at the expense of increased sensitivity to errors in the wavenumber estimate and the computational requirements involved in calculating the Fourier coefficients.

ACKNOWLEDGMENTS

The research described in this paper has been supported, both financially and technically, by Industrial Research Limited. The authors also gratefully acknowledge the financial assistance provided by the New Zealand Foundation for Research, Science and Technology and the New Zealand Vice-Chancellors' Committee Fund. The research was undertaken while the first author held a New Zealand Universities Postgraduate Scholarship.

REFERENCES

1. D. U. Noiseux 1970 *Journal of the Acoustical Society of America* **47**, 238–247. Measurement of power flow in uniform beams and plates.
2. *Proceedings of the* 3*rd International Congress on Intensity Techniques*, 1990, Senlis, France.
3. *Proceedings of the* 4*th International Congress on Intensity Techniques*, 1994, Senlis, France.
4. G. Pavic 1976 *Journal of Sound and Vibration* **49**, 221–230. Measurement of structure borne wave intensity, part 1: formulation of the methods.
5. J. W. Verheij 1980 *Journal of Sound and Vibration* **70**, 133–138. Cross spectral density methods for measuring structure borne power flow on beams and pipes.
6. J. Linjama and T. Lahti 1992 *Journal of Sound and Vibration* **153**, 21–36. Estimation of bending wave intensity in beams using the frequency response technique.
7. P. D. Bauman 1994 *Journal of Sound and Vibration* **74**, 677–694. Measurement of structural intensity: analytic and experimental evaluation of various techniques for the case of flexural waves in one-dimensional structures.
8. H. M. M. van der Wal 1990 *Proceedings of the* 3*rd International Congress on Intensity Techniques*, *Senlis*, *France*, 289–296. Exploratory power flow measurements on a bar.
9. H. Sander 1993 *Proceedings of the* 4*th International Congress on Intensity Techniques*, *Senlis*, *France*, 207–214. On the importance of boundary layers for intensity measurements in beams.
10. K. Shibata, M. Kato, N. Takatsu, O. Wakatsuki and K. Kobayashi 1994 *Proceedings of Inter-Noise* 94, *Yokohama*, *Japan*, 1697–1700. Measuring condition and precision of structural intensity measurement.
11. P. D. Yaylor 1990 *Proceedings of the* 3*rd International Congress on Intensity Techniques*, *Senlis*, *France*, 249–256. Measurement of structural intensity, reflection coefficient, and termination impedance for bending wavein beams.
12. J. L. Trolle and E. Luzzato 1990 *Proceedings of the* 3*rd International Congress on Intensity Techniques*, *Senlis*, *France*, 397–404. Application of structural intensity for diagnostic in one dimension problems.
13. C. R. Halkyard and B. R. Mace 1995 *Journal of Sound and Vibration* **185**, 279–298. Structural intensity in beams—waves, transducer systems and the conditioning problem.
14. L. Cremer, M. Heckl and E. E. Ungar 1988 *Structure-borne Sound*. Berlin: Springer-Verlag; second edition.
15. M. Abramowitz and I. A. Stegun 1984 *Pocketbook of Mathematical Functions*. Frankfurt: Verlag Harri Deutsch.
16. S. Barnett 1971 *Matrices in Control Theory*. London: van Nostrand Reinhold.
17. J. C. Nash 1990 *Compact Numerical Methods for Computers—Linear Algebra and Function Minimalisation*. Bristol: Adam Hilger.
18. C. R. Halkyard 1995 *Ph.D. Thesis*, *University of Auckland*, *New Zealand*. The application of wave based techniques to intensity measurement in beams and plates.

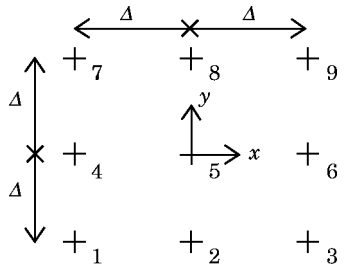

Figure A1. The response locations for finite difference approximation.

APPENDIX 1: FINITE DIFFERENCE APPROXIMATIONS FOR FAR FIELD INTENSITY MEASUREMENT IN PLATES

In the absence of near-fields the intensity in a plate can be expressed in terms of spatial derivatives of displacement of up to second order. If displacement or one of its temporal derivatives is measured at nine locations, as shown in Figure A1, then the required parameters may be approximated as

$$w = w_5, \qquad \frac{\partial w}{\partial x} \approx \frac{w_6 - w_4}{2\Delta}, \qquad \frac{\partial w}{\partial y} \approx \frac{w_8 - w_2}{2\Delta}, \qquad \frac{\partial^2 w}{\partial x^2} \approx \frac{w_4 - 2w_5 + w_6}{\Delta^2},$$

$$\frac{\partial^2 w}{\partial y^2} \approx \frac{w_2 - 2w_5 + w_8}{\Delta^2}, \qquad \frac{\partial^2 w}{\partial x\,\partial y} \approx \frac{w_9 - w_7 - w_3 + w_1}{4\Delta^2}. \tag{A1}$$

APPENDIX 2: LIST OF SYMBOLS

$A(\theta)$	complex wave amplitude as a function of propagation direction	$\mathbf{T}$	transformation matrix
		t	time
C_n	complex Fourier series coefficient	U_n, V_n	related to Bessel functions (see section 5)
$\mathbf{C}$	vector of Fourier coefficients		
D	plate flexural stiffness per unit width	$\mathbf{W}$	vector of measured variables
		$w()$	displacement (in z-direction)
e	base of natural logarithm	$\mathrm{Y}_n()$	nth order Bessel function of the second kind
F	complex force amplitude		
$f(t)$	time harmonic point force	x, y, z	co-ordinates in Cartesian space
$\mathrm{H}_n^{(2)}$	nth order Hankel function of the second kind	x', y', x_0, y_0	displacements in Cartesian space
		α_a, α_s	condition number
h	plate thickness	δ	Dirac delta function
$\mathrm{J}_n()$	nth order Bessel function of the first kind	ε_r	radial strain
		ν	Poisson ratio
k_p	plate wavenumber	ρ	plate density
n	order of Bessel or Hankel function, Fourier index	ω	angular frequency
		θ	propagation direction
$r, \hat{r}, \phi, \hat{\phi}, z$	co-ordinates in polar space		
R, φ, w	displacements in polar space	$\langle\,\rangle$	time average
S	area of integration		